Materials and Design 139 (2018) 181–187

Contents lists available at ScienceDirect

Materials and Design

journal homepage: www.elsevier.com/locate/matdes

High-quality graphene directly grown on Cu nanoparticles for Cu-graphene nanocomposites

Shuangyue Wang [a,b], Shaobo Han [a,c], Guoqing Xin [d], Jianliang Lin [e], Ronghua Wei [e], Jie Lian [d], Kai Sun [c], Xiaotao Zu [a,*], Qingkai Yu [b,*]

[a] Institute of Fundamental and Frontier Sciences, University of Electronic Science and Technology of China, Chengdu 610054, PR China
[b] Ingram School of Engineering, MSEC, Texas State University, San Marcos, TX 78666, USA
[c] Michigan Center for Materials Characterization (MCMC) & Department of Materials Science and Engineering, The University of Michigan, Ann Arbor, MI 48109, USA
[d] Department of Mechanical, Aerospace and Nuclear Engineering, Rensselaer Polytechnic Institute, Troy, NY 12180, USA
[e] Southwest Research Institute, San Antonio, TX 78238, USA

HIGHLIGHTS

- High-quality graphene was directly grown on the surface of Cu nanoparticles via chemical vapor deposition.
- The nanocomposite exhibits a hardness of 2.53 GPa with no distinctive degeneration in electrical resistivity.
- There is a 2 orders of magnitude decrease in wear rate and 175% improvement in coefficient of friction.
- The formation of graphene tribofilm is responsible for the effective protection of Cu matrix from wear.

GRAPHICAL ABSTRACT

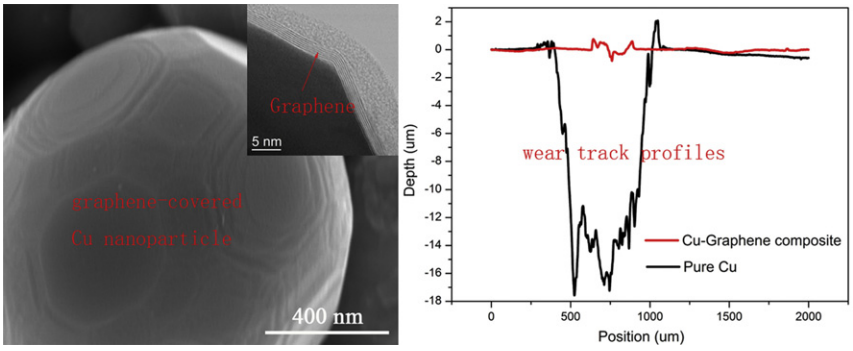

ARTICLE INFO

Article history:
Received 21 June 2017
Received in revised form 3 November 2017
Accepted 4 November 2017
Available online 6 November 2017

Keywords:
High-quality graphene
Cu nanoparticles
Nanocomposite
Superior hardness
Wear resistance

ABSTRACT

High-quality graphene was directly grown on the surface of Cu nanoparticles (NPs) via chemical vapor deposition (CVD) and then the graphene-covered Cu NPs were consolidated into dense Cu-graphene nanocomposites at different temperature. The surface of Cu NPs is well protected from oxidation due to the coverage of graphene. Nanocomposite consolidated at 650 °C (Cu/G-650) exhibits a hardness of 2.53 GPa with no distinctive different electrical resistivity compared with pure Cu, 2 orders of magnitude decrease in wear rate and 175% improvement in the coefficient of friction (COF) were reported for the Cu/G-650 nanocomposite as compared with pure Cu. The formation of graphene tribofilm is attributed for the effective protection of the Cu matrix from wear.

1. Introduction

High performance metal materials with enhanced properties of high specific strength, good thermal conductivity, good wear resistance and corrosion resistance are required to meet the challenges of extreme conditions encountered in diverse industrial applications and increased longevity demand. Metal-based nanocomposites are a potential solution for high comprehensive properties. Graphene is a single-atomic-layer two-dimensional (2D) material with excellent mechanical properties, such as the intrinsic strength of 130 GPa and a Young's modulus of 1TPa [1] as well as high electrical [2] and thermal conductivities [3,4].

* Corresponding authors.
E-mail addresses: xtzu@uestc.edu.cn (X. Zu), qingkai.yu@txstate.edu (Q. Yu).

https://doi.org/10.1016/j.matdes.2017.11.010
0264-1275/

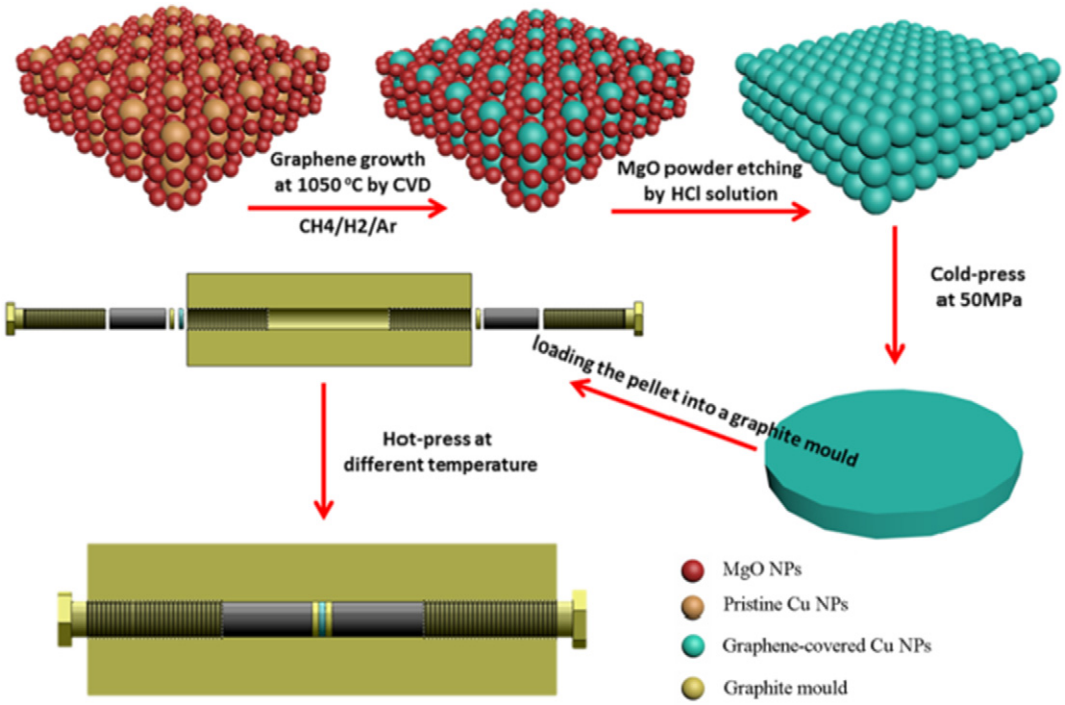

Fig. 1. Schematics of the graphene growth on Cu NPs as well as compressing process for Cu-graphene nanocomposites.

Metal-graphene nanocomposites were recently fabricated by chemical or mechanical integration using reduced graphene oxide (rGO) [5,6] or graphene nanoplatelets [7,8] as the reinforcement agents. However, a wide gap exists between experimental mechanical properties achieved and theoretical predictions [9] for graphene-based metal matrix. The inferior properties of the graphene-based metal matrix can be attributed to multiple reasons including the failure of homogeneous dispersion of graphene flakes in metal matrix, significant thermal damage on graphene during sintering, reaction of metal and graphene into carbides during sintering [10], unavoidable defects in rGO [11],

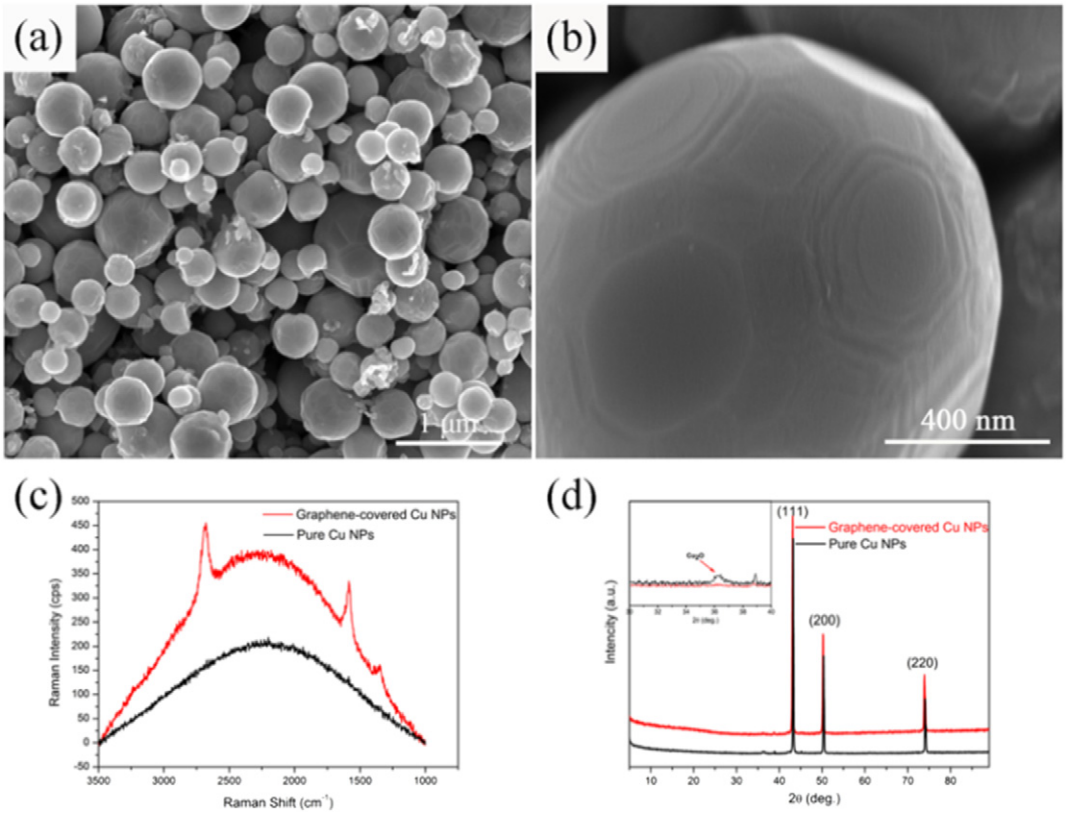

Fig. 2. (a) SEM images of low-magnification and (b) high-magnification graphene-covered Cu NPs. (c) Raman spectrum of graphene-covered Cu NPs and pure Cu NPs after CVD treated. (d) XRD patterns of graphene-covered Cu NPs and pure Cu NPs. Insert in (d) is the enlarged patterns from 30 to 40°.

and weak adhesion between reinforcement materials and matrix [9]. To address these issues, Chen [12] reported in-situ growth of graphene on Cu particles to mitigate the agglomeration of graphene. However, the low-quality of the graphene limited the enhancement on the hardness of Cu. Pavithra [13] utilized pulse reverse electrodeposition to introduce graphene into Cu matrix showing enhanced hardness of 2.5 GPa and an modulus of 137 GPa, as 2 times and 1.2 times higher than these of bulk Cu, respectively. However, this method can only be used for fabricating thin film Cu-graphene nanocomposites with a few hundred micrometers in thickness. To fabricate high-performance Cu-graphene nanocomposites, three main requirements are: i) uniform dispersion of graphene in the matrix; ii) sufficient interface strength between Cu and graphene and iii) low density of defects.

Moreover, its high chemical inertness [14], extreme strength, easy shear capability between layers, and low surface energy [15] make graphene a good candidate for solid lubricants for protecting surface in friction [16]. Berman [17] revealed that a few-layer graphene drastically reduces the wear and the coefficient of friction (COF) of steel during the initial sliding regime and under low load conditions. Kim [18] reported that graphene films effectively reduced the adhesion and friction forces on SiO_2/Si substrate. However, in most of these reports, graphene so far is only applied on the sliding surface rather than on the matrix. Therefore, after the surface is worn with time in friction, the lubrication effect is gone. In addition, according to Peng's work [19], the friction and wear properties are strongly dependent on the quality of graphene. Owing to the low density of defects [20], graphene by chemical vapor deposition (CVD) is naturally a good candidate for the high tribological performance of metal-graphene nanocomposites.

In this research, we report the preparation of Cu-graphene nanocomposites by sintering graphene-covered Cu nanoparticles (NPs), which were obtained by directly growing high-quality graphene on the surface of Cu NPs by CVD. The Cu/G-650 nanocomposite shows hardness of 2.53 GPa, which is approximately 2.5 times higher than pure bulk Cu (1.01 GPa). In addition, the nanocomposite maintains a low electrical resistivity (1.72×10^{-6} Ω-cm) as pure Cu, which can be attributed to the high-quality graphene filled in the copper matrix. The Cu/G-650 nanocomposite also has relatively lower friction coefficient (0.2) compared to that of pure Cu (0.34). More importantly, the wear volume of the nanocomposite is 2 orders of magnitude smaller than that of pure Cu after 2000 cycle tests. Such significant reductions in friction and wear are attributed to the formation of a uniform tribofilm by graphene with low friction energy dissipation at sliding contact interfaces.

2. Experimental

2.1. Fabrication of graphene-covered Cu NPs

Graphene-covered Cu NPs were fabricated by ambient-pressure CVD method. Cu NPs (99.9% pure, 80–100 nm) were used as the resource and graphene grains were grown by CVD (CH_4 as the carbon feedstock) on Cu NPs at ambient pressure. To avoid Cu-grain growth during graphene grown at high temperature, MgO NPs (99% pure, 60–100 nm) were used as spacers. First, Cu NPs and MgO NPs were mixed at a mass ratio of 1:3 by high speed blender (Blender Lab 2 Speed 1 L 120 V, Thomas Scientific) for 30 min; second, the mixture was taken into a quartz tube and then loaded in a CVD furnace to heat up to 1050 °C under 300 sccm Ar

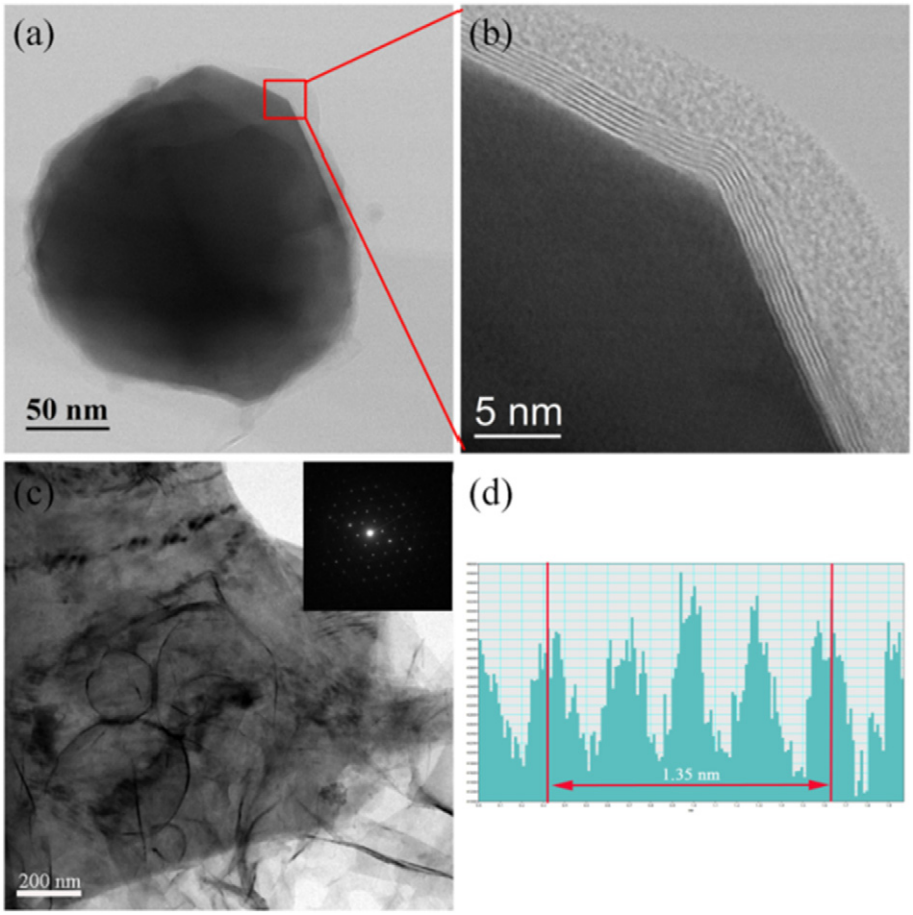

Fig. 3. (a) TEM images of low-magnification and (b) high-magnification graphene-covered Cu NPs. (c) TEM images of the as-obtained graphene after etching Cu NPs, and insert is SAED pattern of the resulting graphene. (d) Profile of the interlayer space of as obtained graphene extracted from (b).

and 100 sccm H_2. The growth was then carried out at 1050 °C for 30 min under a gas mixture 600 sccm diluted (in Ar) CH_4 (concentration 500 ppm) and 10 sccm H_2. Finally, the sample was cooled to room temperature under the protection of Ar. After graphene growth (the mixed NPs shown in Fig. S1a), the MgO NPs were etched by 10% HCl solution to obtain graphene-covered Cu NPs (The schematics of the process shown in Fig. 1). The mechanisms for the selective etching on MgO and Cu are: 1) as the chemical reaction between HCl acid and MgO nanoparticles is much faster than that between HCl acid and Cu nanoparticles, the MgO nanoparticles can be removed quickly; 2) the Cu nanoparticles are covered by multi-layer graphene, which can protect the Cu surface from contacting with HCl acid, so the Cu nanoparticles could avoid being etched.

2.2. Preparation of Cu-graphene nanocomposites

The Cu-graphene nanocomposites were prepared by cold-pressing the graphene-covered Cu NPs to pellets by a 20 T desktop hydraulic laboratory press, and then the obtained pellets were transferred to a designed graphite mold. Finally, the screwed graphite mold were loaded into a CVD furnace for further sintering at 600 °C, 650 °C, 700 °C, and 750 °C for 30 min. The final Cu-Graphene nanocomposites were around10 mm in diameter and 1 mm in thickness.

2.3. Characterizations

The microstructures of the graphene-covered Cu NPs and Cu-Graphene nanocomposites were characterized with scanning electron microscopy (Nova, Nano SEM, FEI), high-resolution transmission electron microscopy (JEM-2010FEF), and Raman microprobe spectroscopy (Thermo Fisher Scientific) with an Ar^+ laser (wavelength 532 nm).

2.4. Performance testing

Vickers hardness and electrical resistivity of Cu-Graphene nanocomposites were tested by a Vickers hardness tester and 4-probe tester, respectively. The as-prepared samples (pure Cu and Cu-graphene samples) were well polished before all performance tests. For wear test, the counterpart was steel ball (E52100 Alloy Steel) with diameter of 0.25 in. The tests were carried out at a load of 1 N, at a speed of 2.74 cm s^{-1} for 2000 cycles and the radius of the wear track was 2.8 mm.

3. Results and discussion

The morphology of a graphene-covered Cu NPs is shown in Fig. 2a,b with different magnifications. The size of graphene-covered Cu NPs is about 10 nm to 1 μm in diameter. It can be seen clearly that the graphene has abundant terraces and step edges duplicating features of Cu surfaces beneath the graphene film [21]. A spherical morphology of graphene after etching Cu NPs is shown in Fig. S1b. For Cu NPs without graphene growth, as shown in Fig. S1c,d, they were severely oxidized owing to no protection on the Cu surface. In contrast, due to the full coverage of multilayer graphene on Cu NPs, the NPs were not oxidized by oxygen in the air (corresponding EDS analysis shown in Fig. S2). The graphene-covered nickel NPs were also prepared by the same method, representative SEM images shown in Fig. S3.

Raman spectrum (Fig. 2c) of graphene-covered Cu NPs shows the characteristic G (1580 cm^{-1}), 2D (2700 cm^{-1}) and D (1350 cm^{-1}) bands of graphene [22,23]. As the profile of D peak reflects the defect density of graphene, the negligible D peak corresponds to very low defect density, indicating that the resulting graphene is of high quality [22]. Fig. 2d shows the XRD patterns of pure Cu and graphene-covered Cu NPs, respectively. Three diffraction peaks with high intensity correspond to (111), (200), and (220) planes of faced centered cubic Cu. No peaks of graphene were observed, which may be due to the strong diffraction peak of Cu that cover up signals from graphene [12]. The enlarged region (insert in Fig. 2d) demonstrated a peak of Cu_2O in the pattern of pure Cu NPs, indicating a slight oxidization of the pure Cu NPs.

According to TEM images as shown in Fig. 3a,b, Cu NPs were fully covered by multilayer (more than 5 layers) graphene with uniform thickness. Further TEM investigation was carried out on the graphene after etching Cu NPs, as shown in Fig. 3c, where the inset SAED pattern indicates high quality of the crystalline structure [24,25]. Interlayer space of graphene film was measured using Digital Micrograph as shown in Fig. 3d. A 1.35 nm thickness for 4 graphene layers indicates the interlayer space of as-grown graphene is 0.34 nm, corresponding to the theoretical value [26]. To our knowledge, this is the first report of growth to such thick layered graphene on a copper substrate. Normally, the growth mechanism for multilayer graphene grown on Cu film is through under-layer formation [27–29] by sharing the same nucleation center. Methane molecules or four intermediates (CH_3, CH_2, CH and C) would rapidly diffuse into the interface between first layer and Cu substrate or penetrate through central defects [27] at high temperature, and finally attach to the edge of the same nucleus to form adlayer graphene. However, owing to the much higher growth rate for the first layer than that of adlayer, in general, the growth of adlayer will

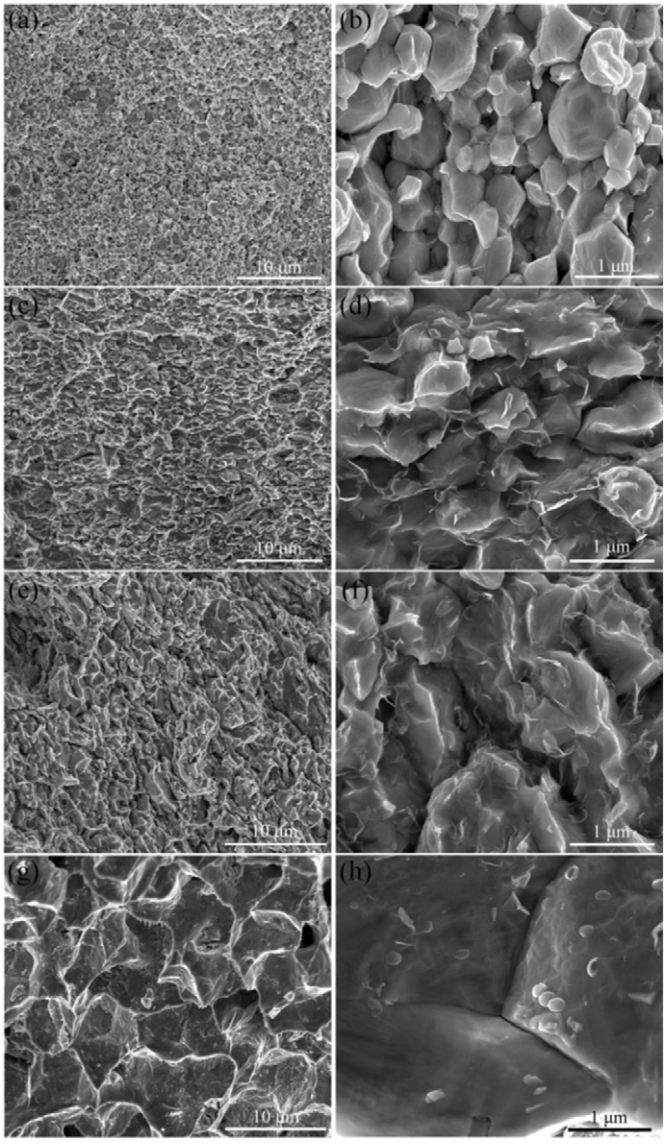

Fig. 4. Fracture surface of Cu-graphene nanocomposites sintered at (a, b) 600 °C, (c, d) 650 °C, (e, f) 700 °C and (g, h) 750 °C, respectively.

Table 1
Vickers hardness of pure Cu and different Cu-graphene nanocomposites.[a]

Materials	Pure Cu-650	Cu/G-600	Cu/G-650	Cu/G-700	Cu/G-750
Hardness (GPa)	1.01	1.88	2.53	2.09	0.90

[a] The last digits in materials names indicate the sintering temperature. For example, the Cu/G-600 denotes Cu-graphene nanocomposite sintered at 600 °C.

terminate once the growth of the first layer is completed. Usually, the size of adlayer is only a few micrometers. In this research, graphene was grown onto the surface of nano-sized copper particles; therefore, the diffusion distance from first layer edge to the growth front of the adlayer is only 10 nm. Thus, these carbon radicals easily arrive at the growth front of the adlayer. Consequently, the Cu NPs were covered with quite thick graphene (more than 5 layers).

The mechanical, electrical, and tribological properties were tested on the sintered pellets (the optical image of the pellet shown in Fig. S4). Fracture surfaces of Cu-graphene nanocomposites sintered at 600 °C, 650 °C, 700 °C, and 750 °C for 30 min are shown in Fig. 4. At low temperature (600 °C) (Fig. 4a,b), graphene is homogeneously dispersed throughout the Cu grain boundaries without agglomeration. During sintering under high pressure and temperature, the Cu grains in the Cu-graphene nanocomposite pellets would undergo extensive plastic deformation, leading to the extrusion of Cu from the graphene film. Therefore, the surfaces of adjacent Cu grains can bond together to form a well-sintered dense pellet [30]. The similar phenomena also occurred in powder metallurgy of aluminum composites [31,32]. As shown in Fig. 4c,d, at 650 °C, Cu grains were elongated, and some graphene films were peeled off to expose bare Cu surfaces. Cu grains bond together, but no grain coarsening occurs. With temperature increasing, the Cu grains are severely coarsened owing to the interdiffusion of Cu atoms at the interface as shown in Fig. 4e–h for the Cu-graphene nanocomposites sintered at 700 and 750 °C, respectively. Despite the grain coarsening at temperatures above 650 °C, the graphene film is still uniformly distributed in Cu matrix. It is also noticed that the deep consecutive dimples with an average diameter of 5 μm appeared at 750 °C, exhibiting ductile micromechanisms of fracture, similar to pure copper [33].

The Vickers hardness of pure Cu and different Cu-graphene nanocomposites were tested and listed in Table 1. The hardness of Cu-graphene nanocomposites increases significantly as compared with pure Cu. Among the nanocomposites, Cu/G-650 exhibits a hardness of 2.53 GPa, 2.5 times higher than that of pure Cu-650. However, the hardness for Cu/G-700 and Cu/G-750 drastically decreases, maybe attributing to the severe coarsening of copper-grains at high temperatures. The mechanism for the hardness enhancement may mainly be attributed to the blockage of dislocation sliding by graphene at the interface between Cu grains and graphene films. The extremely high shear strength of graphene can effectively hurdle the propagation of dislocations between grains (the shear modulus of zigzag and armchair structures to be 0.213 and 0.228 TPa, respectively [33]). In our Cu-graphene nanocomposites, the multilayered graphene (more than 5 layers) is rigid sufficiently to pile up dislocations in a Cu grain instead of sliding across the grain boundary [34].

The XPS spectra of Cu-graphene nanocomposites at different sintering temperature show two Cu peaks at binding energies of 932.6 and 952.5 eV, which correspond to $Cu2p_{3/2}$ and $Cu2p_{1/2}$ [35,36]. The peaks at 933.6 and 953.4 eV correspond to CuO (Fig. 5a). Fig. 5b shows the deconvoluted C1s spectra of the Cu-graphene nanocomposites at different sintering temperature. The peak consists of two components, one at binding energy 284.7 eV which features the C═C sp^2 bonds in the graphitic network, one at 285.6 eV which is attributed to carbon bonds with sp^3 hybridization respectively [37–39]. The intensity of the sp^3 components increased with the sintering temperature increasing, indicating that the filled graphene began to become amorphous and oxidized. The transformation was attributed to the high pressure at higher temperature. At 750 °C, the component of sp^3 has reached 18.6%, resulting the intrinsic strength of graphene degenerated severely. That is one of the reasons why the hardness decreased seriously at 750 °C.

Electrical measurement and tribology testing were performed on the Cu/G-650 nanocomposite showing the highest hardness. The resistivity of G/Cu-650 sample measured by four-point probe method is approximately 1.72×10^{-6} Ω-cm, similar to that of Pure Cu-650 (1.69×10^{-6} Ω-cm), as a result of the superior-quality graphene by CVD. The friction and wear experiments were performed on a wear testing machine using a ball-on-disc configuration in a circular motion mode [34]. Fig. 6a–d present the wear tracks of Pure Cu-650 and Cu/G-650 nanocomposite against steel ball (E52100 Alloy Steel) under 1 N sliding load under dry condition for 2000 cycles. The width of the wear track is approximately 770 μm and 185 μm for pure Cu-650 and Cu/G-650 samples, respectively. For Pure Cu-650 (Fig. 6a,b), adhesive craters and ploughing scratches were observed obviously, and large amount of debris appeared at the wear area, indicating that the wear mechanism for pure Cu against steel ball is dominantly adhesive wear and abrasive wear [40,41]. After the test, the roughness of the wear track increases markedly, indicating seriously wear loss. For the Cu/G-650 nanocomposite (Fig. 6c,d), the wear track is much narrower than that of pure Cu samples. Moreover, the wear damage was mild with very little wear mark and significant less wear debris in and around the sliding wear scar and track areas. Finally, the surface of wear area of the Cu/G-650 nanocomposite is much smoother than that of pure Cu.

The dramatic reduction in wear can be attributed to the presence of graphene layers within the sliding wear track as confirmed by EDS and Raman spectroscopy (shown in Fig. S5a,b). Graphene forms a uniform tribofilm within the wear area, reduces the wear friction between the sample and the counterpart ball, and thus improves the wear resistance. An important benefit of the Cu-graphene nanocomposite is that the high-quality graphene dispersed into the whole Cu matrix can constantly feed stock for the tribofilm. The elemental line scan analysis shows that the wear track was fully covered with graphene (Fig. S5c,d). The

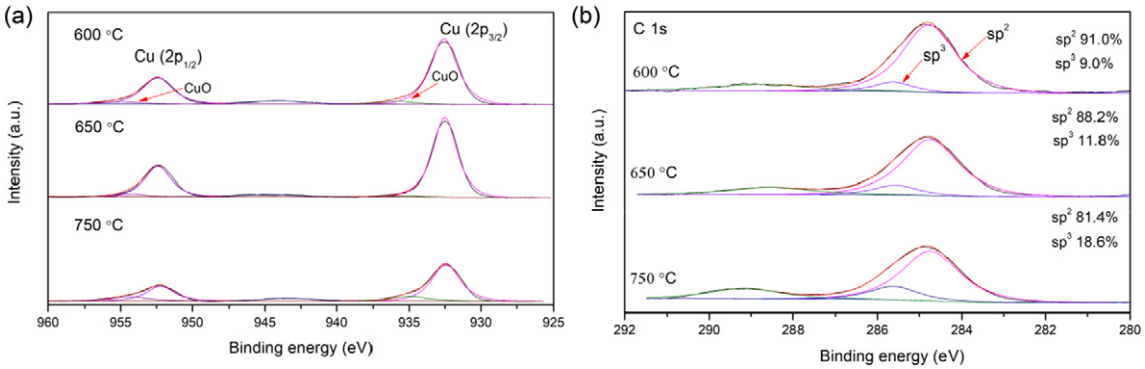

Fig. 5. XPS core-level (a) Cu2p and (b) C1s spectra of the Cu-graphene nanocomposites at different sintering temperature.

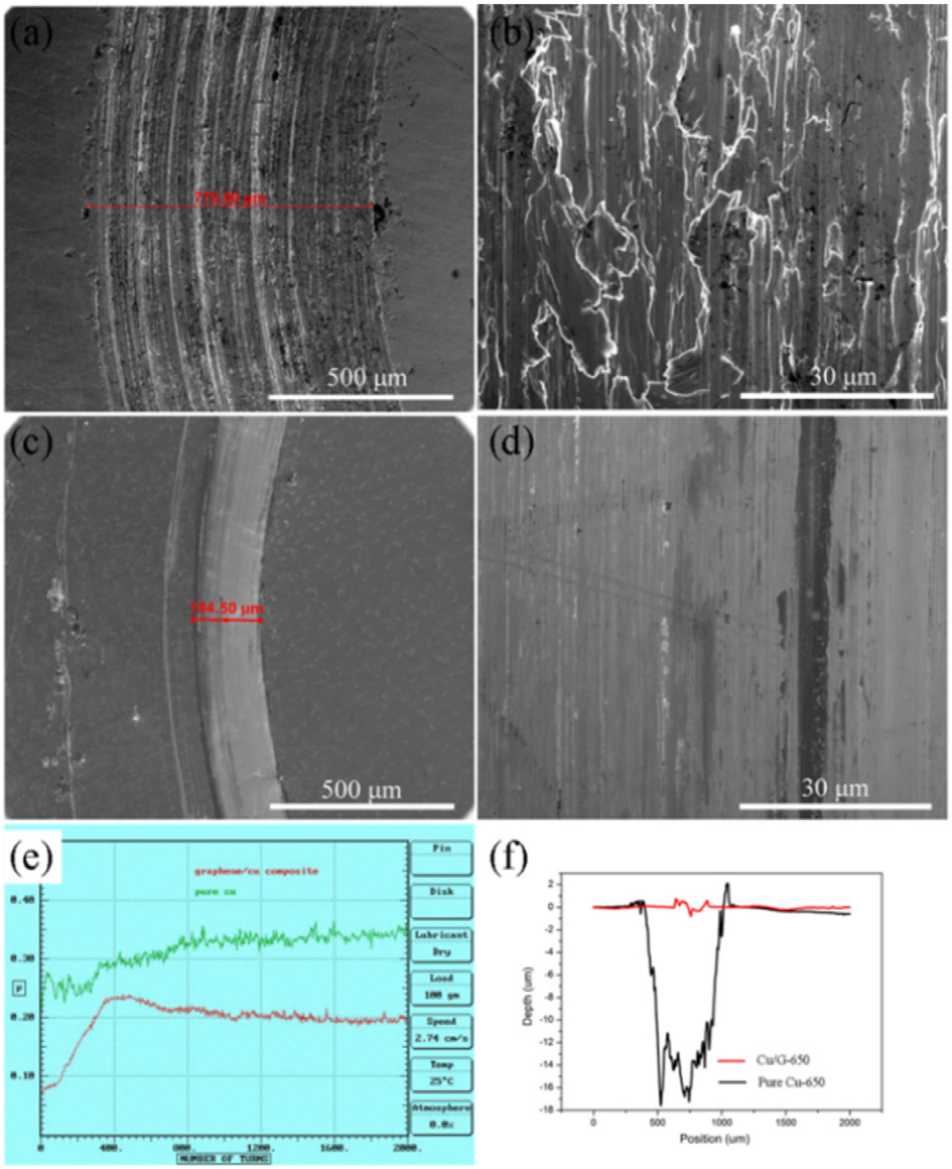

Fig. 6. SEM micrograph of wear tracks of (a, b) pure Cu-650. (c, d) Cu/G-650 nanocomposite against alloy steel ball at 1 N sliding load under dry condition. (e) Coefficients of friction (ν) of pure Cu-650 and Cu/G-650 nanocomposite. (f) Corresponding wear track profiles of pure Cu and Cu/G-650 nanocomposite.

COFs of pure Cu-650 and Cu/G-650 nanocomposite are shown in Fig. 6e. The friction behavior of pure Cu-650 is unsteady and increased gradually due to adhesive wear. The COF during the later stage reached a value of 0.35. However, for the nanocomposite, the COF is lower than that of pure Cu with a value of 0.2 and the friction behavior is steady at the later stage. After the completion of the sliding test of 2000 cycles, the graphene becomes defective and disordered during the sliding tests, resulting in a significant reduction of 2D peak intensity in the Raman spectrum measured in the wear scar (Fig. S5b). Furthermore, a 3D surface profilometer was utilized to investigate the wear tracks. The line scans profiles of the wear tracks are shown in Fig. 6f. For pure Cu, the depth and width of the wear track are 16 μm and 750 μm, respectively, corresponding to the SEM images (Fig. 6a,b). However, for Cu-graphene nanocomposites, the wear damage is slight and the depth and width are 1 μm and 180 μm, respectively. Calculated wear volume and wear rate were listed in Table 2. The presented values of the wear show that G/Cu-650 sample can reduce wear by 2 orders of magnitude compared with pure Cu after the 2000-cycle tests. The graphene with excellent graphitic structure and strong van der Waals forces between the layers can effectively distribute the high pressure among the layers [19]. The high substrate stiffness due to the very thick graphene covered can decrease the friction energy dissipation [42]. Then Cu-graphene nanocomposites can remain relatively effective at reducing friction and resisting wear under high pressure.

Table 2
Wear volume and wear rate calculations after 2000 cycle tests at 1 N load.

Materials	Calculated wear Volume (mm^3)	Wear rate (Wear / (load·distance)) (mm^3 / N·m)
Pure Cu-650	133×10^{-3}	379.4×10^{-5}
Cu/G-650	0.98×10^{-3}	2.8×10^{-5}

4. Conclusions

In conclusion, high quality graphene was directly grown on Cu NPs by CVD and directly consolidated into dense graphene-Cu nanocomposites showing enhanced mechanical strength and tribological properties. TEM and Raman spectrum show the as-grown graphene is of high

quality comparable to that of CVD graphene on Cu substrate. The Cu/G-650 nanocomposite shows a hardness of 2.53 GPa, around 2.5 times enhancement compared with pure Cu while exhibiting an electrical conductivity comparable to that of pure Cu. The tribological properties of the Cu-graphene composites were investigated using a ball-on-disc technique. The value of COF decreases from 0.35 to 0.2. The wear volume of the nanocomposite is 2 orders of magnitude smaller than that of pure Cu for 2000 cycle tests. We attribute the hardness enhancement as well as the superior tribological behavior to the homogeneous dispersion of high-quality graphene into Cu matrix.

Acknowledgments

Funding: This work was supported by financial support from the NSAF Joint Foundation of China [U1630126]; the US National Science Foundation under the award of CMMI [1463083].

Appendix A. Supplementary data

Supplementary data to this article can be found online at https://doi.org/10.1016/j.matdes.2017.11.010.

References

[1] A. Sakhaee-Pour, Elastic properties of single-layered graphene sheet, Solid State Commun. 149 (2009) 91–95.
[2] S.V. Morozov, K.S. Novoselov, M.I. Katsnelson, F. Schedin, D.C. Elias, J.A. Jaszczak, A.K. Geim, Giant intrinsic carrier mobilities in graphene and its bilayer, Phys. Rev. Lett. 100 (2008).
[3] A.A. Balandin, S. Ghosh, W. Bao, I. Calizo, D. Teweldebrhan, F. Miao, C.N. Lau, Superior thermal conductivity of single-layer graphene, Nano Lett. 8 (2008) 902–907.
[4] Y.L. Tang, P. Peng, S.Y. Wang, Z.H. Liu, X.T. Zu, Q.K. Yu, Continuous production of graphite nanosheets by bubbling chemical vapor deposition using molten copper, Chem. Mater. 29 (2017) 8404–8411.
[5] J. Hwang, T. Yoon, S.H. Jin, J. Lee, T.S. Kim, S.H. Hong, S. Jeon, Enhanced mechanical properties of graphene/copper nanocomposites using a molecular-level mixing process, Adv. Mater. 25 (2013) 6724–6729.
[6] M. Rashad, F.S. Pan, H.H. Hu, M. Asif, S. Hussain, J. She, Enhanced tensile properties of magnesium composites reinforced with graphene nanoplatelets, Mater. Sci. Eng. A 630 (2015) 36–44.
[7] W.J. Kim, T.J. Lee, S.H. Han, Multi-layer graphene/copper composites: preparation using high-ratio differential speed rolling, microstructure and mechanical properties, Carbon 69 (2014) 55–65.
[8] S.Y. Wang, G.K. Wang, X. Zhang, Y.L. Tang, J.W. Wu, X. Xiang, X.T. Zu, Q.K. Yu, Novel flower-like graphene foam directly grown on a nickel template by chemical vapor deposition, Carbon 120 (2017) 103–110.
[9] Y. Tang, X. Yang, R. Wang, M. Li, Enhancement of the mechanical properties of graphene-copper composites with graphene-nickel hybrids, Mater. Sci. Eng. A 599 (2014) 247–254.
[10] C. Gomez-Navarro, J.C. Meyer, R.S. Sundaram, A. Chuvilin, S. Kurasch, M. Burghard, K. Kern, U. Kaiser, Atomic structure of reduced graphene oxide, Nano Lett. 10 (2010) 1144–1148.
[11] K. Chu, C. Jia, Enhanced strength in bulk graphene-copper composites, Phys. Status Solidi A 211 (2014) 184–190.
[12] Y.K. Chen, X. Zhang, E.Z. Liu, C.N. He, C.S. Shi, J.J. Li, P. Nash, N.Q. Zhao, Fabrication of in-situ grown graphene reinforced Cu matrix composites, Sci. Rep. 6 (2016) 9.
[13] C.L.P. Pavithra, B.V. Sarada, K.V. Rajulapati, T.N. Rao, G. Sundararajan, A. New Electrochemical, Approach for the synthesis of copper-graphene nanocomposite foils with high hardness, Sci. Rep. 4 (2014).
[14] S. Chen, L. Brown, M. Levendorf, W. Cai, S.-Y. Ju, J. Edgeworth, X. Li, C.W. Magnuson, A. Velamakanni, R.D. Piner, J. Kang, J. Park, R.S. Ruoff, Oxidation resistance of graphene-coated Cu and Cu/Ni alloy, ACS Nano 5 (2011) 1321–1327.
[15] S. Wang, Y. Zhang, N. Abidi, L. Cabrales, Wettability and surface free energy of graphene films, Langmuir 25 (2009) 11078–11081.
[16] D. Berman, A. Erdemir, A.V. Sumant, Graphene: a new emerging lubricant, Mater. Today 17 (2014) 31–42.
[17] D. Berman, A. Erdemir, A.V. Sumant, Few layer graphene to reduce wear and friction on sliding steel surfaces, Carbon 54 (2013) 454–459.
[18] K.-S. Kim, H.-J. Lee, C. Lee, S.-K. Lee, H. Jang, J.-H. Ahn, J.-H. Kim, H.-J. Lee, Chemical vapor deposition-grown graphene: the thinnest solid lubricant, ACS Nano 5 (2011) 5107–5114.
[19] Y. Peng, Z. Wang, K. Zout, Friction and wear properties of different types of graphene nanosheets as effective solid lubricants, Langmuir 31 (2015) 7782–7791.
[20] X.S. Li, W.W. Cai, J.H. An, S. Kim, J. Nah, D.X. Yang, R. Piner, A. Velamakanni, I. Jung, E. Tutuc, S.K. Banerjee, L. Colombo, R.S. Ruoff, Large-area synthesis of high-quality and uniform graphene films on copper foils, Science 324 (2009) 1312–1314.
[21] Z.-J. Wang, G. Weinberg, Q. Zhang, T. Lunkenbein, A. Klein-Hoffmann, M. Kurnatowska, M. Plodinec, Q. Li, L. Chi, R. Schloegl, M.-G. Willinger, Direct observation of graphene growth and associated copper substrate dynamics by in situ scanning electron microscopy, ACS Nano 9 (2015) 1506–1519.
[22] L.M. Malard, M.A. Pimenta, G. Dresselhaus, M.S. Dresselhaus, Raman spectroscopy in graphene, Phys. Rep.-Rev. Sec. Phys. Lett. 473 (2009) 51–87.
[23] A.C. Ferrari, J.C. Meyer, V. Scardaci, C. Casiraghi, M. Lazzeri, F. Mauri, S. Piscanec, D. Jiang, K.S. Novoselov, S. Roth, A.K. Geim, Raman spectrum of graphene and graphene layers, Phys. Rev. Lett. 97 (2006) 4.
[24] H. Sun, J. Xu, C. Wang, G. Ge, Y. Jia, J. Liu, F. Song, J. Wan, Synthesis of large-area monolayer and bilayer graphene using solid coronene by chemical vapor deposition, Carbon 108 (2016) 356–362.
[25] J.C. Meyer, A.K. Geim, M.I. Katsnelson, K.S. Novoselov, T.J. Booth, S. Roth, The structure of suspended graphene sheets, Nature 446 (2007) 60–63.
[26] Z.Z. Sun, Z. Yan, J. Yao, E. Beitler, Y. Zhu, J.M. Tour, Growth of graphene from solid carbon sources, Nature 468 (2010) 549–552.
[27] H. Zhao, Y.-C. Lin, C.-H. Yeh, H. Tian, Y.-C. Chen, D. Xie, Y. Yang, K. Suenaga, T.-L. Ren, P.-W. Chiu, Growth and raman spectra of single-crystal trilayer graphene with different stacking orientations, ACS Nano 8 (2014) 10766–10773.
[28] S. Nie, W. Wu, S. Xing, Q. Yu, J. Bao, S.-s. Pei, K.F. McCarty, Growth from below: bilayer graphene on copper by chemical vapor deposition, New J. Phys. 14 (2012).
[29] Q. Li, H. Chou, J.-H. Zhong, J.-Y. Liu, A. Dolocan, J. Zhang, Y. Zhou, R.S. Ruoff, S. Chen, W. Cai, Growth of adlayer graphene on Cu studied by carbon isotope labeling, Nano Lett. 13 (2013) 486–490.
[30] J.M. Liang, C. Kong, M.Z. Quadir, Y.F. Zheng, X. Yao, P. Munroe, D.L. Zhang, Microstructure and mechanical properties of a bulk ultrafine grained Al-7Si-0.3Mg alloy produced by thermomechanical consolidation of a nanocrystalline powder, Mater. Sci. Eng. A 658 (2016) 192–202.
[31] E.J. Lavernia, B.Q. Han, J.M. Schoenung, Cryomilled nanostructured materials: processing and properties, Mater. Sci. Eng. A 493 (2008) 207–214.
[32] J.J. Fuentes, J.A. Rodriguez, E.J. Herrera, Increasing the ductility and strength of submicrometer-grained P/M aluminium, J. Alloys Compd. 484 (2009) 806–811.
[33] Y.-g. Liao, X.-q. Han, M.-x. Zeng, M. Jin, Influence of Cu on microstructure and tensile properties of 7XXX series aluminum alloy, Mater. Des. 66 (2015) 581–586.
[34] Y. Kim, J. Lee, M.S. Yeom, J.W. Shin, H. Kim, Y. Cui, J.W. Kysar, J. Hone, Y. Jung, S. Jeon, S.M. Han, Strengthening effect of single-atomic-layer graphene in metal-graphene nanolayered composites, Nat. Commun. 4 (2013).
[35] A. Pendashteh, M.F. Mousavi, M.S. Rahmanifar, Fabrication of anchored copper oxide nanoparticles on graphene oxide nanosheets via an electrostatic coprecipitation and its application as supercapacitor, Electrochim. Acta 88 (2013) 347–357.
[36] Y.J. Mai, X.L. Wang, J.Y. Xiang, Y.Q. Qiao, D. Zhang, C.D. Gu, J.P. Tu, CuO/graphene composite as anode materials for lithium-ion batteries, Electrochim. Acta 56 (2011) 2306–2311.
[37] Stuart T. Jackson, Ralph G. Nuzzo, Determining hybridization differences for amorphous carbon from the XPS C 1s envelope, Appl. Surf. Sci. 90 (1995) 195–203.
[38] A. Siokou, F. Ravani, S. Karakalos, O. Frank, M. Kalbac, C. Galiotis, Surface refinement and electronic properties of graphene layers grown on copper substrate: an XPS, UPS and EELS study, Appl. Surf. Sci. 257 (2011) 9785–9790.
[39] S.F. Wang, G.Z. Sun, L.M. Fang, L. Lei, X. Xiang, X.T. ZuX, A comparative study of ZnAl2O4 nanoparticles synthesized from different aluminum salts for use as fluorescence materials, Sci. Rep. 5 (2015).
[40] R.G. Zheng, X.M. Liu, Effect of load and velocity on wear behaviour of Cu based self-lubricating composite, Mater. Res. Innov. 18 (2014) 12–15.
[41] R. Ritasalo, M. Antonov, R. Veinthal, S.-P. Hannula, Comparison of the wear and frictional properties of Cu matrix composites prepared by pulsed electric current sintering, Proc. Est. Acad. Sci. 63 (2014) 62–74.
[42] H. Zhang, Z. Guo, H. Gao, T. Chang, Stiffness-dependent interlayer friction of graphene, Carbon 94 (2015) 60–66.